Monitoring surface charge migration in the spectral dynamics of single CdSe/CdS nanodot/nanorod heterostructures

J. Müller, J. M. Lupton,* A. L. Rogach, and J. Feldmann
Photonics and Optoelectronics Group, Physics Department and CeNS, Ludwig-Maximilians-Universität, Amalienstr 54, 80799 Munich, Germany

D. V. Talapin and H. Weller
Institute of Physical Chemistry, University of Hamburg, Grindelallee 117, 20146 Hamburg, Germany
(Received 12 August 2005; published 29 November 2005)

Spherical CdSe nanocrystals capped by a CdS rod-like shell exhibit interesting spectral dynamics on the single particle level. Spectral boxcar averaging reveals a high degree of correlation between the emission energy, spectral linewidth, phonon coupling strength, and emission intensity of the single nanocrystal. The results can be described in terms of a spatially varying surface charge density in the vicinity of the exciton localized in the CdSe core, leading to a quantum confined Stark effect which modifies the transition energy and the radiative rate. Whereas internal charging of the particle results in a change in the nonradiative rate, surface charges primarily influence the radiative rate. Additionally, we observe characteristic spectral dynamics in frequency space, the magnitude of which depends slightly on temperature and strongly on excitation density. By distinguishing between continuous spectral jitter and discrete spectral jumping associated with a reversible particle ionization event, we can attribute the spectral dynamics to either a slowly varying surface charge density or a rapidly occurring polarization change due to a reversible expulsion of a charge carrier from the semiconductor nanostructure. Whereas the former exhibits universal Gaussian statistics, the latter is best characterized by a Lorentzian noise spectrum. The Gaussian spectral noise increases with spectral redshift of the emission and with increasing proximity of the surface charge to the localized exciton. The observation of a high degree of correlation between peak position and linewidth right up to room temperature suggests applications of the nanocrystals as extremely sensitive single charge detectors in both solid state devices and in biomolecular labeling, where highly local measurements of the dielectric environment are required. Nanoscale control of the physical shape of nanocrystals provides a versatile test bed for studying electronic noise, making the approach relevant to a wide range of conducting and emissive solid state systems.

DOI: 10.1103/PhysRevB.72.205339 PACS number(s): 78.66.Hf, 73.63.Kv, 61.46.+w, 78.67.Hc

I. INTRODUCTION

The spectroscopy of individual low-dimensional semiconductor nanostructures opens up a window to the intrinsic electronic properties of quantum-confined structures unperturbed by disorder.[1–5] This limitation of fluorescence to the ultimate level of single photons[2] reveals sensitive reactions of elementary photoexcitations to the immediate environment.[3–5] Single molecules, for example, and indeed any two-level system in the solid state can act as highly sensitive reporters on nanoscale polarizations,[6–10] providing a rough qualitative or even quantitative understanding of the influence of the environment on the emitter is available. Molecules can change their conformation in the solid state, even at the lowest temperatures, leading to subtle changes in the emission properties.[11] Alternatively, the environment can fluctuate, a scenario particularly prominent in amorphous polymeric matrices, and alter the molecular transition dipole moment.[9] Dark state formation such as triplets,[11] free radicals,[12] or charge separated states[13,14] can further modify the fluorescence and lead to pronounced intermittency in the emission. Although similar effects are observed for semiconductor nanocrystals[15] (NCs), the origin of emission dynamics both in terms of emission energy and intensity is not as straightforward to pinpoint.[3–5] Fluorescence blinking has recently attracted considerable attention,[16–25] as it constitutes a serious problem when employing NCs as fluorescence labels in biophysical applications,[26,27] and is also of interest in epitaxially vapor phase grown quantum dots.[28] The standard model advocated to explain blinking in these particles relates to reversible charging effects due to the expulsion of a charge carrier[4,17,20,24] from the NC. Subsequent excitation leads to an efficient Auger-type three-particle relaxation, which dominates over the weakly allowed spontaneous emission and leads to an apparent fluorescence intermittency.[16,29] Reversible expulsion of a carrier from the NC modifies the immediate dielectric environment of the particle,[4] which is elegantly manifested in the correlation between photoluminescence (PL) intermittency and spectral diffusion, the spectral jitter observed in the emission.[16] While low temperature measurements, in particular, can yield valuable information on spectral diffusion and changes in the polarization of the environment, most studies tend to focus on the room temperature PL intermittency. Spectral diffusion in NCs is thought to arise from a net surface charge density, which creates a permanent polarization experienced by the particle and thus induces an internal electric field.[4,30] Similar spectral shifts are observed during spectral diffusion as are under application of an external electric field.[31] Indeed, a few investigations exist in general on the influence of strong elec-

tric fields on low-dimensional semiconductor structures.[31–40] Whereas the quantum-confined Stark effect is generally associated with quantum wells,[41] which allow efficient electrostatic wave function manipulation and penetration into the barrier layer, lower-dimensional materials with stronger confinement should be less prone to efficient Stark shifts. However, as the volume of the quantum dot is small and a significant fraction of the atoms constituting the nanostructure sit on the surface potentially perturbed by surface charges, extremely high local fields may be experienced. These can even lead to exciton ionization.[42] To date, however, it has not been possible to correlate apparently random spectral shifts with changes in fluorescence intensity, which would provide a direct signature of field induced exciton screening and changes in the radiative rate analogous to the conventional situation in quantum wells.[43]

Besides the reversible photoinduced charging of the particle[4,44] leading to Auger-type nonradiative recombination,[29] permanent charges also exist on the surface of the particle. These originate from dangling bonds unsaturated by the surface ligands.[4,21,45–52] Although little is known about the precise energetics of these surface traps,[48] a number of rather different experimental techniques speak in favor of their presence, such as dielectric spectroscopy,[46] electric force microscopy[49] (EFM), and PL microscopy.[4] The paradigm that particle charging itself ultimately leads to inhibition of spontaneous emission is incorrect, as a net charge may also be situated on the particle surface without enhancing Auger recombination. Charged particles observed in EFM may, therefore, turn out to be emissive. Very interestingly, a further source of net charging was recently identified in CdSe nanorods[53] using EFM. Distortions of the ionic lattice are believed to be the cause of a net polarization anisotropy observed, which gives rise to giant dipole moments.[53,54] Elongated nanoparticles[55] are particularly interesting material systems to study the interplay between net polarization and spectral dynamics as the spherical symmetry is broken. This leads to a spatially asymmetric system with a preferential axis for charge density anisotropy.[56]

We recently demonstrated that elongated particles consisting of a near spherical CdSe core with an epitaxially attached CdS nanorod exhibit a universal correlation between the peak fluorescence energy and the spectral linewidth on the single particle level.[56] This correlation arises due to the fact that net surface charge induces a Stark shift of the emission energy in dependence of the distance to the CdSe core holding the exciton. Spatial jitter of the charge density leads to line broadening in the single particle[4,57,58] PL, which substantially exceeds the homogeneous linewidth at low temperatures.[59] The closer the charges are situated to the emissive core of the particle, the stronger the effect of the spatial jitter will be on spectral broadening. In the present work, we substantiate these initial observations further by demonstrating that a straightforward data analysis of the single particle emission yields a universal correlation between the spectral peak position and the fluorescence linewidth, intensity, and phonon coupling. These observations are all consistent with the picture of surface charges inducing a quantum-confined Stark effect,[4,60–66] but also provide direct evidence that the local field effect actually modifies the radiative rate and thus the emission intensity. Most importantly, we show that the strength of the spectral jitter, which follows a universal Gaussian noise pattern,[16,56] depends sensitively on the spatial separation of surface charges from the emissive CdSe core. Spectral noise analysis, therefore, provides a direct way of imaging and tracking surface charges

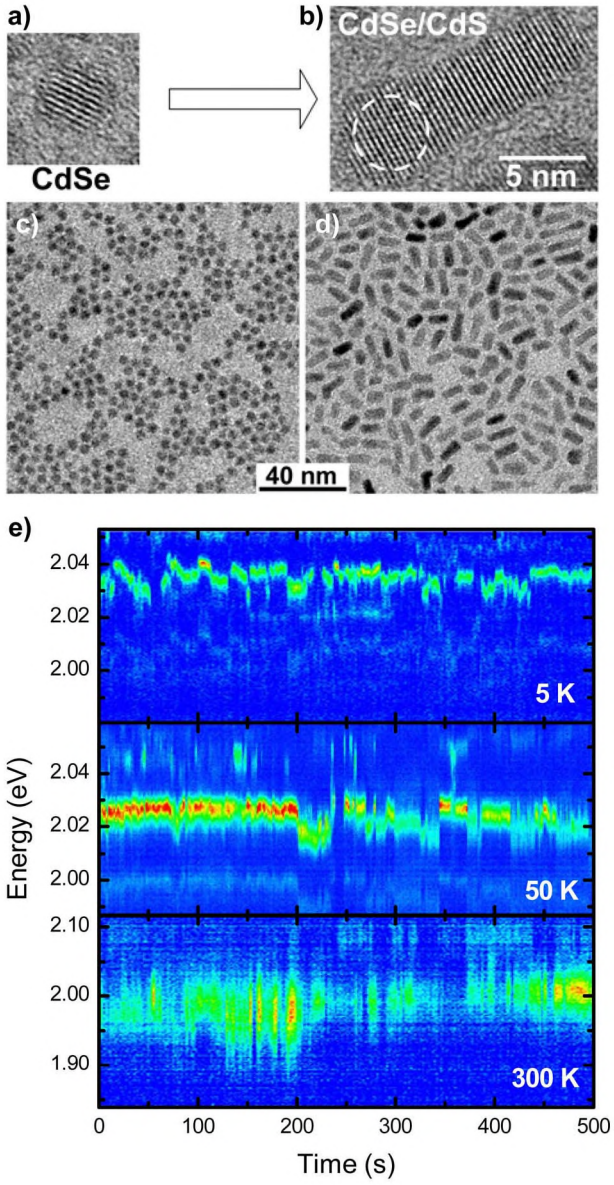

FIG. 1. (Color online) (a)–(d) Transmission electron microscopy images of 4 nm CdSe NCs [(a),(c)] and elongated CdSe/CdS nanohererostructures [(b),(d)] formed by epitaxial growth of CdS nonorods on the $\{00\bar{1}\}$ facets of CdSe nanocrystals. The location of the emitting CdSe core inside the CdSe/CdS nanoheterostructure is indicated by a dashed circle in (b). (e) Spectral diffusion in the fluorescence of single elongated CdSe/CdS nanocrystals at 5 K, 50 K, and 300 K. The PL spectra are plotted as a function of time in a two-dimensional representation with the intensity encoded in color/gray scale (blue/very dark gray: low intensity, red/dark gray: high intensity). The temporal resolution of the data is 1 s.

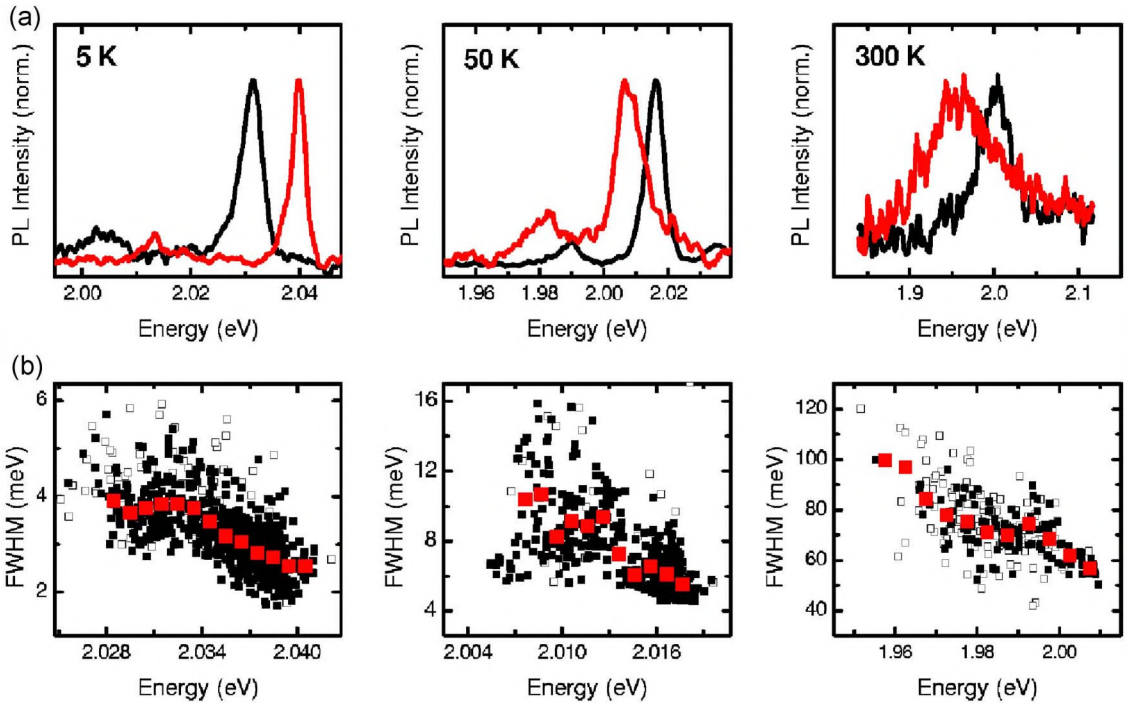

FIG. 2. (Color online) Correlation between peak position and peak linewidth for three different particles recorded at 5 K, 50 K, and 300 K. (a) Two representative spectra taken from the traces in Fig. 1, illustrating a spectral broadening concomitant with the spectral redshift. (b) Correlation between spectral linewidth and peak position. The open squares correspond to the raw data. The solid squares represent filtered data sets, in which only spectral shifts were considered which occur on time scales longer than the measurement resolution of 1 s. The large solid squares indicate a binned average.

on semiconductor nanostructures right up to room temperature.

II. EXPERIMENT

The elongated nanorods employed have previously been discussed in detail.[67] They consist of a spherical CdSe core covered by an elongated rod-like CdS shell grown epitaxially on the $\{00\bar{1}\}$ facet of the hexagonal phase CdSe core and are stabilized by hexadecylamine, tri-*n*-octylphosphine oxide and tri-*n*-octylphosphine ligands in chloroform. Figures 1(a)–1(d) show transmission electron microscopy images of CdSe NCs and elongated CdSe/CdS nanoheterostructures. The interference pattern in Fig. 1(b) reveals the high degree of crystal quality of the nanostructure. The NCs were diluted to a $\sim 10^{-10}$ molar concentration and mixed with polystyrene (5 mg/ml). Spin coating on Si wafers covered with 300 nm SiO_2 at 5000 rpm yielded films $\sim$25 nm thick with an average interparticle spacing of 5 μm. The samples were mounted in a Helium cold finger microscope cryostat and excited nonresonantly at 457.9 nm using the circularly polarized light of an Ar ion laser with a typical spot size of 80 μm corresponding to an excitation density of 50 W/cm^2. Excitation was performed in an epifluorescence dark field configuration at an angle of incidence of 60° to the normal. The single particle PL was collected using a long working distance microscope objective lens of numerical aperture 0.55. This provided a spatial resolution of 800 nm, allowing facile spatial isolation of single NCs at 5 μm interparticle spacing. The PL was spectrally filtered using a long pass interference filter (AHV Analysetechnik AG, Tübingen, Germany) with a cutoff at 545 nm to remove scattered excitation light, passed through a 0.3 m monochromator with a maximal spectral resolution of $\sim$0.4 meV and subsequently imaged onto a cooled front-illuminated charge coupled device (Sensicam QE, PCO AG, Kelheim, Germany). Spectral time traces were recorded with a temporal resolution of 1 s. The elongated NCs are characterized by particularly large absorption cross sections,[67] which in turn lead to high emission intensities. We recorded typical emission intensities of 1000 counts/s for our rod-like particles at an overall detection efficiency of $\sim$2%. Spherical CdSe (CdS) core (shell) particles, in contrast, yielded on average 200 counts/s and were found to be much more prone to blinking and substantial spectral jumps during the spectral diffusion. The number of emitting spots detected in the fluorescence microscope scaled directly with the particle concentration, whereas the average emission intensity per spot remained independent of concentration and exhibited only a weak scatter from particle to particle. These observations demonstrate that indeed only isolated nonaggregated particles are observed.

III. RESULTS

A. Spectral dynamics

Single NCs exhibit a pronounced temporal variation both in terms of the PL intensity and the PL wavelength. The variation of the emission is best illustrated in a two-

dimensional representation of the fluorescence energy as a function of time, where the PL intensity is color encoded. Figure 1(e) illustrates the PL spectra as a function of time for three typical particles recorded at 5 K, 50 K, and 300 K. At low temperatures, the emission exhibits a high degree of stability in terms of intensity, while nevertheless substantial spectral fluctuations occur. PL intermittency becomes more probable with increasing temperature, which also leads to a substantial spectral broadening of the single particle PL. The spectral range of ~20 meV covered by the particle during spectral diffusion only increases slightly with temperature. Two types of spectral dynamics can be distinguished loosely: those occurring without a noticeable change in intensity, and those coinciding with a large modulation in intensity or even an intermittency event.[16] Note that due to the finite integration time, a PL intermittency of less than 1 s duration will simply result in a reduction but not a complete disappearance of the PL. Strong intermittency events coincide with large spectral jumps and have previously been associated with discrete ionization and subsequent neutralization events.[16] Although the signal to noise ratio decreases with increasing temperature, we are nevertheless able to extract individual PL spectra at different times. These are shown in the upper panel of Fig. 2. At low temperatures, the PL spectra consist of a narrow zero phonon line followed by the discrete 27 meV LO phonon of CdSe. The phonon line merges with the purely electronic transition at higher temperatures. Two representative spectra are given for each temperature in Fig. 2. Generally, it is seen that the redder of the two spectra appears broader. By fitting Lorentzian lines to each spectrum of the entire trace shown in Fig. 1, we are able to extract the peak position and linewidth for each measurement and plot the linewidth in dependence of the peak position. Figure 2(b) illustrates that a clear correlation exists between the peak position and the PL linewidth at each temperature. The open squares indicate the raw data taken directly from Fig. 1. Although the raw data do clearly display a correlation, the scatter remains substantial. This is due to the fact that the limited temporal resolution of the setup averages over spectral dynamics on time scales shorter than 1 s. Spectral switching on such time scales may, therefore, lead to an imprecise fitting estimate of the peak position or a spectral smearing and thus an overestimate of the linewidth. To minimize the effect of charge motion and spectral diffusion *during* the measurement, we next consider only spectral shifts which occur on time scales longer than 1 s and discard data points for which the drift in peak position between the preceding and the subsequent spectra is larger than 2 meV. The remaining 70% of data points are shown by the solid black squares in Fig. 2(b) and exhibit considerably less scatter on the full width at half maximum (FWHM) axis. The red squares indicate the average of the data set over peak position binned in intervals of 1 meV at 5 K and 50 K and 5 meV at 300 K, which further reduces the scatter.

A simple way to remove the temporal noise is to sort the spectra with respect to peak position and thus remove the time dimension. In effect, this corresponds to spectral boxcar averaging. The benefit of this approach, which requires no manipulation of the raw spectra, is clearly seen in Fig. 3, which shows two plots of normalized fluorescence spectra

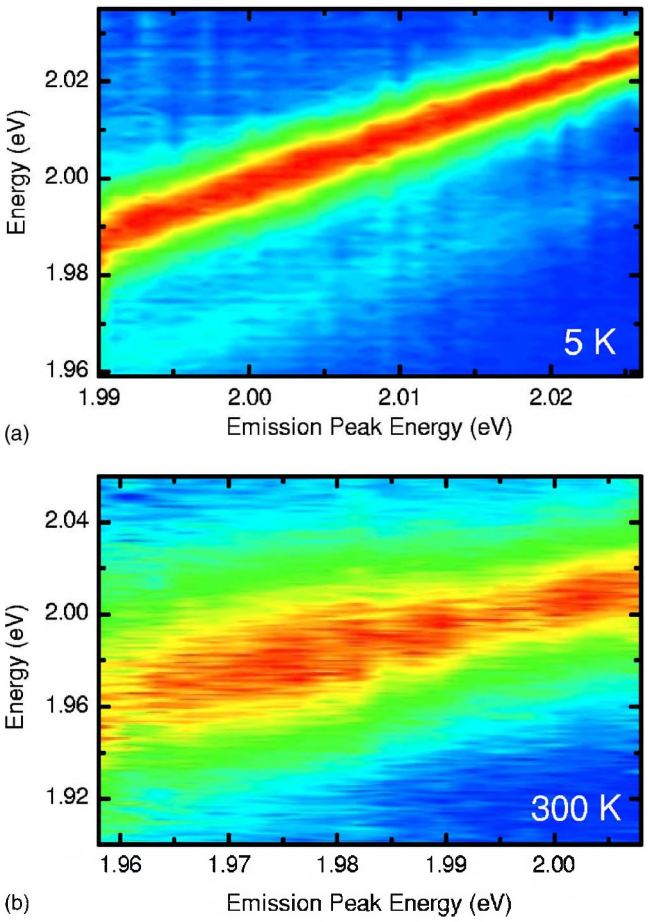

FIG. 3. (Color online) PL spectra of one single NC recorded during the spectral diffusion process and sorted by peak energy. As the peak energy shifts to the red, the LO phonon sideband increases in intensity and the spectra broaden, giving rise to a funnel-like shape of the graph (a). (b) The effect is also visible at room temperature, although the phonon sideband can no longer be resolved. A redshift in the emission results in an unambiguous spectral broadening.

against central peak position at 5 K and 300 K. The sorted traces at 5 K shown in Fig. 3(a) clearly illustrate how the emission broadens as the transition shifts to the red. Simultaneously, the phonon band follows the emission to lower energies, but increases in intensity toward the red while remaining discrete from the purely electronic transition. The effect of spectral broadening upon redshifting of the emission is slightly less pronounced at the higher temperatures because of the overall broader spectra, but is all the same clearly visible. The sorted 300 K spectra exhibit considerably more noise and a less uniform intensity due to the reduced signal-to-noise level apparent from the raw spectra shown in Fig. 2. Sorting the room temperature spectra with regards to the spectral fluorescence maximum nevertheless clearly manifests the increase in spectral width with increasing redshift of the emission, a signature of the unique geometrical structure[56] of the NC.

The sorted spectra now allow a much more facile and accurate extraction of the spectral parameters such as the linewidth, the phonon coupling strength, and the PL inten-

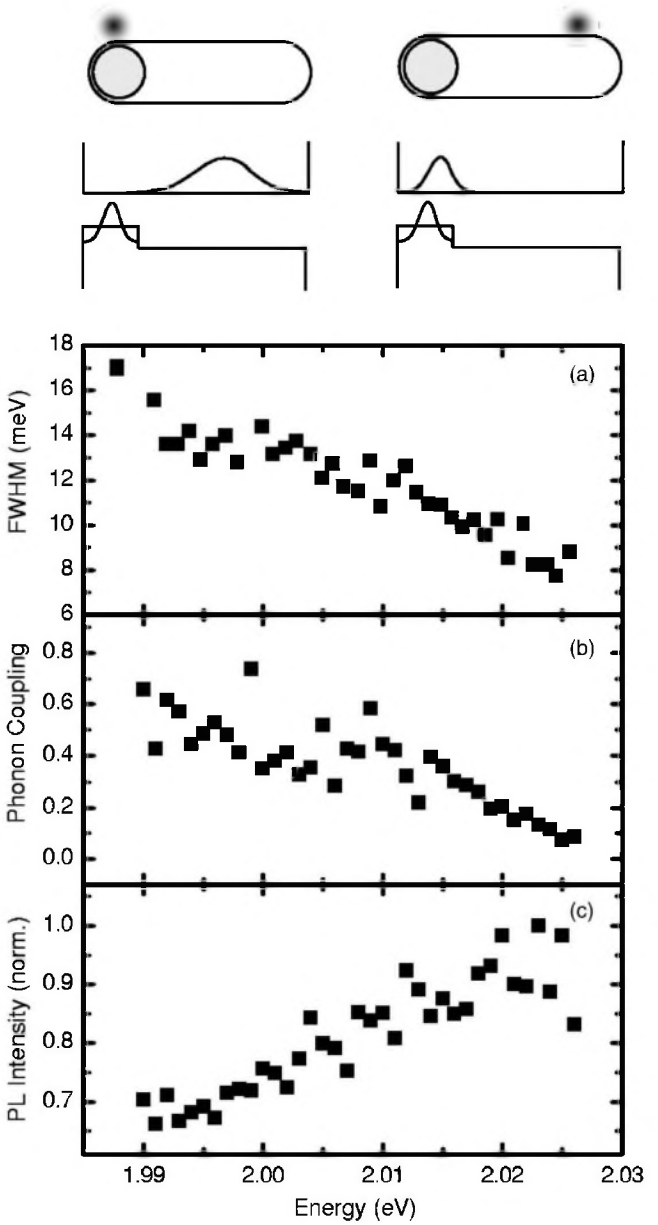

FIG. 4. Correlation between fluorescence peak position and linewidth (FWHM), phonon coupling strength, and PL intensity for the sorted spectral trace measured at 5 K and shown in Fig. 3(a). Sorting of the spectra allows us to bin related spectra prior to fitting and extracting the linewidth, peak position, phonon coupling, and intensity. The scheme illustrates the mechanism responsible for the correlations, explained in more detail in Fig. 10. Briefly, the hole is confined in the CdSe core, whereas the electron is free to penetrate the CdS shell. Surface charges modify the overlap of the electron and hole wave functions, which in turn control FWHM, phonon coupling, peak energy, and PL intensity.

sity, as a number of similar spectra can be averaged prior to extracting the spectral information. Rather than fitting to a single spectrum and subsequently averaging the fit values as in Fig. 2, this prior averaging dramatically reduces the uncertainty on the fit. Figure 4 displays the linewidth (FWHM), phonon coupling, and PL intensity as a function of the mean emission energy. The further in the blue the emission from

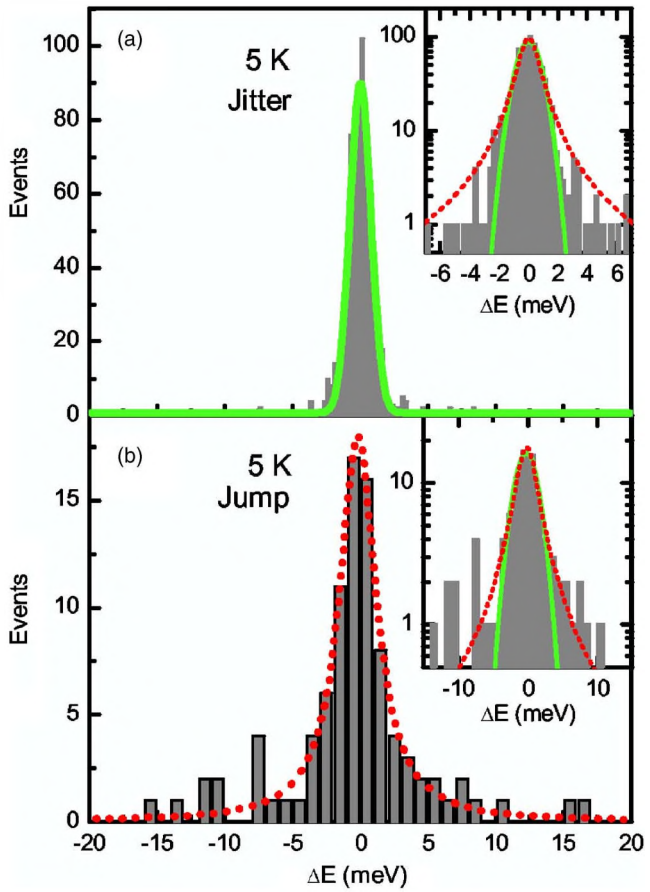

FIG. 5. (Color online) Spectral diffusion statistics of the PL trace shown in Fig. 1(a). The histograms illustrate the difference in energy ΔE between two subsequent spectral peaks. (a) Overall trace consisting of 800 events. (b) Events interrupted by fluorescence intermittency (total of 90). The insets show the histograms on a logarithmic scale with a Gaussian (solid line) and a Lorentzian (dotted line) superimposed.

the single NC occurs, the narrower the electronic transition, the weaker the LO phonon intensity relative to the main PL band and the stronger the overall emission intensity. The scheme in Fig. 4 illustrates the influence of surface charges on the electron-hole wave function overlap, which is discussed in more detail later on. The hole is localized on the CdSe core, whereas the electron can penetrate the CdS shell. A change in surface charge density modifies the electron-hole wave function overlap of the nanostructure and thus the measurement parameters discussed in the figure.

B. Statistics of spectral diffusion

The temporal dynamics of the emission can be investigated further by considering the statistics of the energetic difference ΔE between two subsequent spectral maxima. Figure 5 shows the analysis of the spectral diffusion of a particle emitting at 5 K. A rough differentiation can be made between spectral shifts occurring between two spectra with and without a substantial (>30%) modulation in the PL intensity.[16] Whereas the first case, which will be referred to

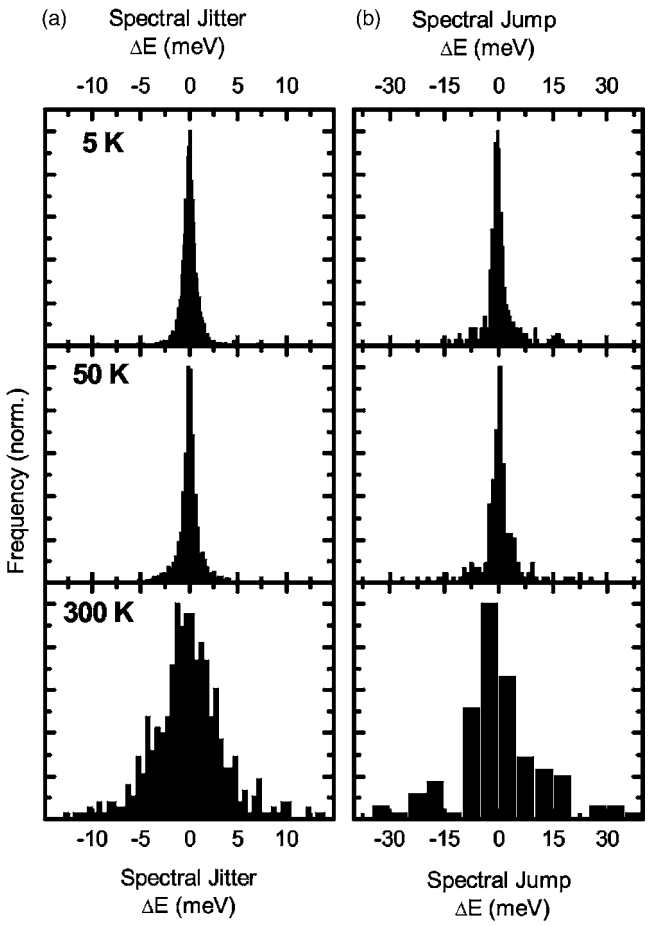

FIG. 6. Temperature dependence of the spectral diffusion statistics. (a) Cumulative ΔE distribution extracted during continuous emission of 15 (5 K), 17 (50 K), and 16 (300 K) single particles. (b) ΔE distribution extracted from energetic jumps following a blinking event.

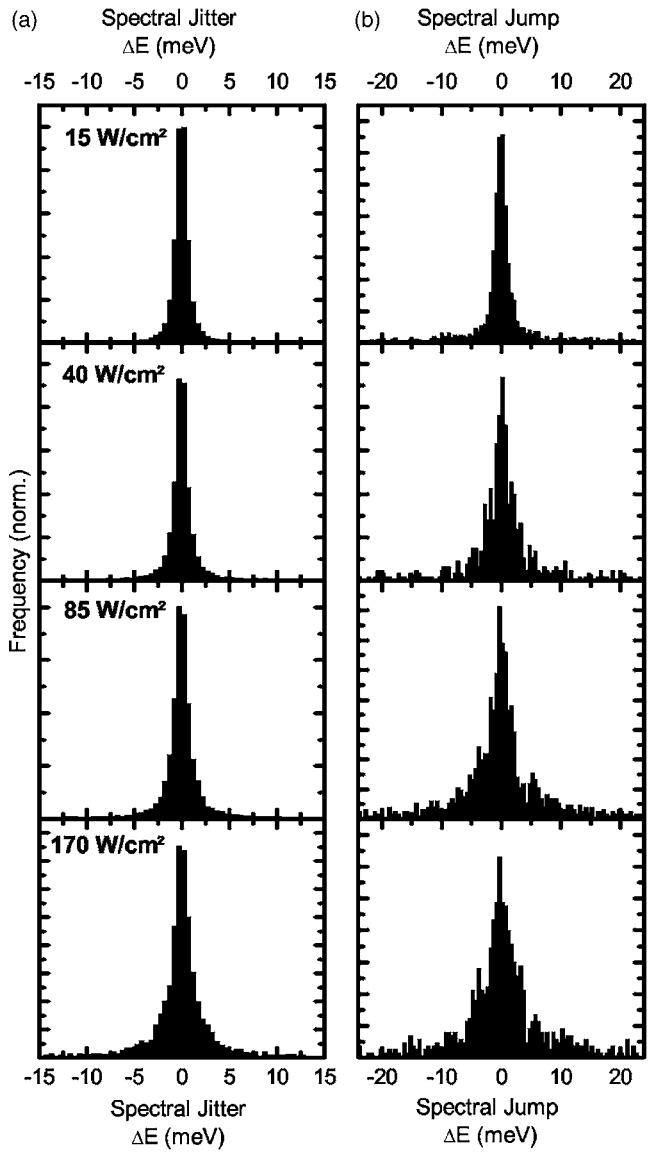

FIG. 7. Intensity dependence of spectral diffusion at 5 K. (a) Cumulative ΔE distribution extracted from 18 single particles during continuous emission. (b) ΔE distribution extracted from energetic jumps following a blinking event.

as spectral jitter, corresponds to $\Delta E = E_{\mathrm{peak},n+1} - E_{\mathrm{peak},n}$, the second case (spectral jumping) is calculated as $\Delta E = E_{\mathrm{peak},n+\tau} - E_{\mathrm{peak},n}$, where τ marks the duration the NC spends in an "off" state and n indicates the index of the measurement. Figure 5(a) shows the ΔE histogram of the spectral jitter. Strictly speaking, it is neither accurately described by a Gaussian nor by a Lorentzian, as becomes apparent when plotting the histogram on a logarithmic scale. In contrast, Fig. 5(b) plots the spectral jumping distribution. Although this histogram has fewer data points, the distribution appears much less consistent with a Gaussian and can be approximated by a Lorentzian.

The statistics of spectral jitter and spectral jump provide a convenient way of characterizing the spectral dynamics in dependence of temperature and excitation intensity. Figure 6 compares spectral jitter [panel (a)] and spectral jump [panel (b)] histograms extracted from the spectral dynamics of a number of different single particles at 5 K, 50 K, and 300 K. The histograms comprise 16 particles at 5 K, 5 NCs at 50 K, and 5 NCs at 300 K with a total of 5600, 7000, and 3600 spectra, respectively. The spectral jitter does not change noticeably with temperature between 5 K and 50 K and can be characterized by the widths of the histograms of 1 meV, 1 meV, and 5 meV for 5 K, 50 K, and 300 K, respectively. The spectral jump histograms are generally substantially broader than the spectral jitter histograms and broaden with increasing temperature from 2 meV (5 K) over 3 meV (50 K) to 10 meV (300 K).

The differentiation between spectral jitter and jumping is equally helpful in understanding the influence of the photoexcitation process on the spectral dynamics of the single particle. Figure 7 shows the cumulative ΔE histograms extracted from 18 single NCs (characterized by over 1000 spectra each) at four different excitation intensities between 15 and 170 W/cm^2. Both jitter and jump histograms broaden with increasing excitation density, but the increase is much stronger for the spectral jump than for the spectral jitter. The results are summarized in Fig. 8, which shows the average histogram width as a function of excitation density. Whereas

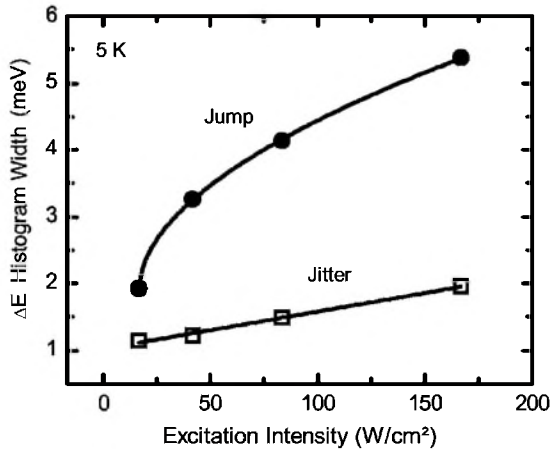

FIG. 8. Dependence of the width of the ΔE histogram in both continuous spectral diffusion (circles) and discrete spectral switching (squares) for an average of 18 single particles at 5 K.

the spectral jitter increases linearly over an order of magnitude in excitation density, the width of the spectral jump histogram appears to follow a strongly sublinear (square root) dependence on intensity. This is illustrated by the fit in the figure. Spectral diffusion exhibits only a weak temperature dependence in the region below 50 K, but increases strongly with excitation density. Above 50 K, there is a substantial thermal influence on the two components of spectral diffusion. We therefore conclude that at low temperatures, spectral diffusion is not a thermal, but a primarily photoinduced process,[4] which is sometimes also referred to as photochemical hole burning.[6]

Finally, we demonstrate that the fluorescence peak-linewidth correlation also directly controls the *statistics* of spectral diffusion. Figure 9 shows the plot of linewidth versus peak energy at 5 k taken from Fig. 2(b). We arbitrarily section the plot into three regions labeled 1 to 3. The corresponding spectral jitter ΔE histograms are given in Fig. 9(b). The histograms are accurately described by a Gaussian. The further in the blue the single particle emits during the spectral diffusion process, the narrower the ΔE_{Jitter} histogram becomes. Figure 9(c) shows the ΔE_{Jitter} histogram from Sec. III on a logarithmic scale. The spectrally selected ΔE histogram follows a Gaussian distribution much more accurately than the entire trace considered in Fig. 5.

IV. DISCUSSION

The results presented in this work provide conclusive evidence for the picture that surface charges control the spectral dynamics of single semiconductor[4] NCs and strongly suggest relevance of these phenomena to semiconductor nanostructures in general.[61,64,65] By breaking the symmetry of the particle by placing the hole trapping CdSe core at one end of the NC and growing an elongated shell on top, a preferential direction for the redistribution of surface charge is given.[56] A surface charge can be situated either close to or far away from the CdSe core or be entirely absent. A charge on the surface of the particle leads to the appearance of an effective

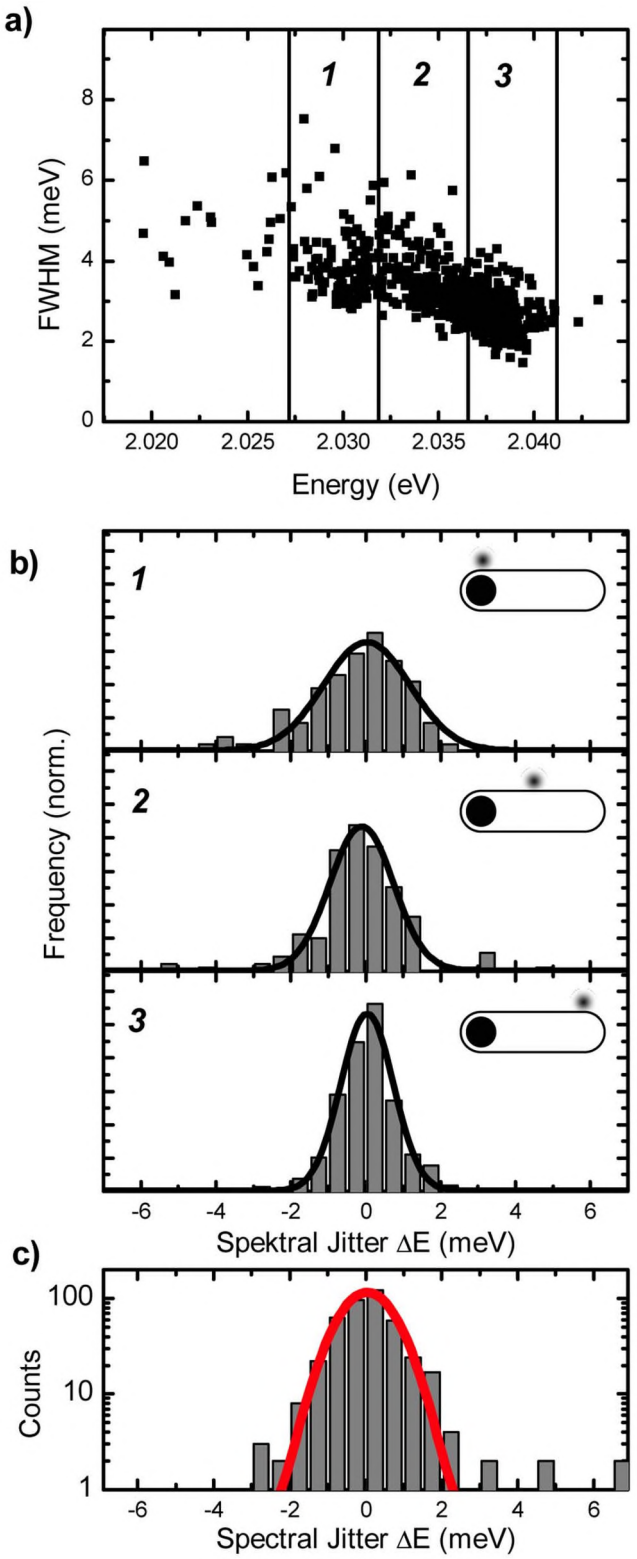

FIG. 9. (Color online) Dissection of the spectral diffusion of a single NC at 5 K into three regions, depending on the magnitude of the Stark effect. (a) The linewidth-peak energy correlation appears continuous and is arbitrarily divided into three equally large regions. (b) ΔE histograms of the continuous spectral diffusion (blinking events discarded) of the three regions indicated in panel (a). (c) ΔE distribution of Sec. 3 shown on a logarithmic scale with a Gaussian superimposed.

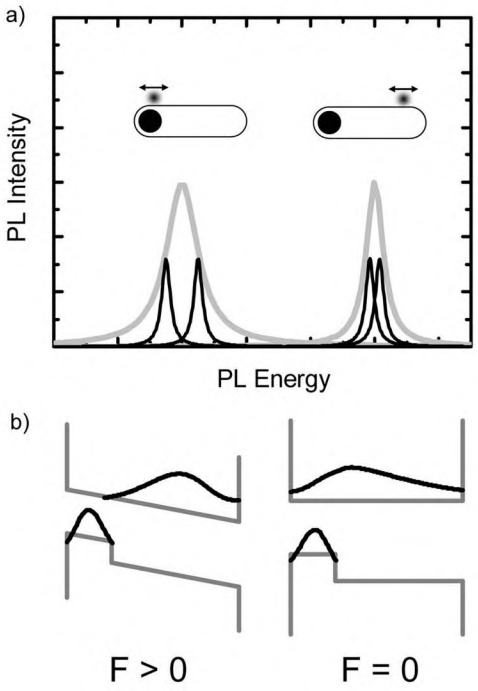

FIG. 10. Schematic representation of the influence of surface charge density on the emission from a single elongated NC. (a) Surface charge present at two different distances from the hole trapping core of the NC results in different magnitudes of a Stark shift in the emission. As the detection of the emission spectrum occurs over a finite time, spatial jitter in the charge density will result in spectral broadening. The closer the surface charge is located to the core of the NC, the stronger the redshift and the stronger the line broadening. (b) The electric field F induced by the surface charge also results in a perturbation of the electron-hole wave function overlap within the NC and thus of the radiative rate. A large local electric field leads to a displacement of the electron with respect to the hole and, therefore, reduces the wave function overlap and the radiative rate, leading to a reduction in PL intensity under the premise of constant nonradiative decay.

electric field, which is readily detected in scanning electric force microscopy.[50] The electric field gives rise to a tilting of the electronic barriers between CdSe core and CdS shell and thus leads to a deformation of the carrier wave function.[4,41] Whereas the hole is confined in the core of the particle, the electron wave function can freely penetrate into the shell. The electron-hole wave function distribution, which controls both the confinement energy and the radiative rate,[41] is consequently extremely sensitive to (negative) surface charges. A surface charge located close to the core will push electron and hole apart in the CdSe core, reducing the confinement energy and thus leading to a redshift of the emission and a reduction in the radiative rate (emission intensity). The further away the surface charge is situated from the core, the weaker the effect of the field induced by the charge will be on the optical transition. The degree of spectral redshift, therefore, provides a measure of the spatial position and magnitude of surface charge. Furthermore, we can also consider the fluorescence linewidth. As the spectral measurement occurs over a finite time, yet there is no reason to assume that surface charges remain spatially stationary during this time, the magnitude of spectral redshift will vary during the integration. This spectral variation will be stronger, the greater the field experienced by the core is. The effect is summarized schematically in Fig. 10, which shows a sketch of two different conceivable spatial positions of surface charge and resulting spectral redshifts and broadening. Additionally, we have also sketched the lowest state electron-hole wave functions, whose overlap decreases with increasing proximity of surface charge to the NC core [panel (b)].

This demonstration of a direct correlation between spectral position, i.e., Stark shift, and fluorescence intensity provides evidence that spectral diffusion primarily controls the radiative rather than the nonradiative rate. This is in stark contrast to molecules, where changes in intensity occurring concurrently with spectral changes originate from a modification of nonradiative channels (such as internal conversion due to vibrational coupling).[8] Surface charges in NCs do not introduce a direct quenching channel. This is in contrast to internal charges within ionized particles, which accelerate nonradiative decay.[29]

The unique correlation between peak position, linewidth, and intensity observed in Fig. 4, therefore, can be understood accurately in terms of this qualitative model. In particular, the high degree of correlation between spectral redshift and emission intensity strongly suggests that the absorption of the particle does not change during spectral diffusion, as absorption occurs into a quasicontinuum of states.[68] This is in stark contrast to single molecules, where spectral diffusion is generally studied in PL excitation, leading to the molecular absorption drifting in and out of resonance with the laser.[69] We note that the changes in wave function distortion giving rise to the spectral dynamics may also originate from a change in magnitude of the surface charge situated at a constant spatial position. While we cannot deconvolve the spatial position and the magnitude of surface charge, we stress that the spectral signatures do provide direct insight into fluctuations in surface charge *density*. Shim *et al.*, however, previously argued that Coulombic repulsion should prevent multiple charging of a single facet[46] of a NC. Furthermore, the linear scaling of the NC permanent dipole moment with radius was also interpreted as a signature for single occupation of charge trap sites on the surface of the particle.[46] As we do not observe any discrete jumps in the peak position-linewidth-intensity correlation, and the correlations all appear to follow one single straight line, we conclude that the surface charge density is governed predominantly by the location rather than the number of carriers and most likely arises from one single carrier.[46]

The field originating from a nonzero surface charge density also strongly modifies the strength of optical phonon coupling. Electric fields are known to enhance phonon coupling in ionic crystals[4] such as CdSe. This has also previously been elegantly demonstrated in single spherical CdSe NCs by applying external electric fields.[4] Increasing the field strength leads to a separation of electron and hole wave functions and the creation of an effective internal field within the NC. This internal field in turn distorts the ionic crystal lattice, the distortion becoming stronger the farther the electron

and hole become separated. The stronger lattice distortion during the existence of the excitonic state is directly measured in terms of an increased coupling to optical phonons, the Fröhlich phonons.[4] The strength of phonon coupling, therefore, provides a fourth parameter besides spectral redshift, linewidth, and intensity to assess the strength of electric fields induced by surface charges in the vicinity of the NC core.

These four experimental quantities are effectively static in nature, as they form a unique quadruplet for each individual spectral measurement. The spectral dynamics themselves, however, also hold signatures of the dynamic change in surface charge density. The larger the spectral redshift in the NC emission, i.e., the stronger the electric field experienced by the exciton, the greater the spectral jitter ΔE_{Jitter} in the emission (Fig. 9). This result is consistent with our assumption that the average spatial change in charge density (also referred to as spatial charge oscillations[4]) with time is independent of the position and magnitude of charge density.

The direct observation of charging of the NC surface has implications for a number of branches of materials and semiconductor science, but may also help to understand and minimize dephasing mechanisms in more exotic systems such as Josephson junction qubits. Whereas self-assembled quantum dots grown epitaxially from the vapor phase on the surface of semiconductors can be charged multiply by application of a gate potential while remaining emissive,[32] the much smaller volume of colloidal quantum dots dramatically enhances nonradiative Auger recombination upon charging.[29,44] The charged state of the NC only becomes visible when the radiative rate is accelerated through field enhancement effects.[44] Nevertheless, spatial fluctuations of charges located either in the bulk holding the quantum dot or on the quantum dot surface can impact immediately on the PL of the single two-level system without quenching it entirely.

Manifestations of fluctuations of trapped charges observed in optical or electrical properties have been reported in many systems ranging from bulk metallic and semiconducting samples,[70] single electron transistors,[71] carbon nanotubes,[72] micronscale semiconductor structures outside of the quantum confinement limit,[73] and Josephson junction qubits.[74,75] Even the magnetic dipole moment of a single quantum dot exhibits fluctuations due to coupling between carriers and magnetic ions, which is manifested in a dynamic Zeeman effect.[76] In all cases, interactions with trapped charges lead to a modulation of either the energy levels experienced by a single charge or the polarization formed through the spatial separation of electron and hole in an optical excitation. In larger systems, such as metallic conductor strips,[70] single electron transistors,[71] or Josephson junctions,[74] the noise detected in the current transported or the voltage induced can be directly related to microscopic defects formed on the surface of the structure during the lithographic sample fabrication process. Understanding the influence of trapped charges in the vicinity of nanoscale systems is, therefore, of great importance. The direct correlation between *spectral noise* signatures and *physical shape* of the particle provided for the first time in our elongated NCs shows how noise can be put to work as a spectroscopic tool to yield insight into the intrinsic nature and the immediate dielectric environment of nanoscale structures. The extreme sensitivity of NCs to charges also suggests that we will be able to employ them as nanoscale optical charge sensors in the future to study single electron transfer processes. A number of recent reports have demonstrated that electron transfer can indeed be studied with single molecules by considering both the fluorescence lifetime and the PL intensity.[7,13,77] Expanding this by the spectral component availed by the giant charge response of colloidal quantum dots is expected to provide new insight into single electron transfer processes occurring, for example, in organic light-emitting diodes.[77] The facile processability of semiconductor NCs from organic solvents in combination with a range of organic semiconductors makes these structures ideal nanoscale probes to explore microscopic electronic processes occurring in devices.

Elongated NCs also provide an interesting model system for single chromophores on conjugated polymers,[78,79] which are equally characterized by a spatially delocalized though more strongly correlated electron system. We have previously shown that conjugated polymers exhibit similar spectral diffusion dynamics, typically governed by a Gaussian distribution of spectral jitter.[78,79] Interestingly, the crossover from single to multiple chromophore emission in conjugated polymers leads to the transition of the ΔE distribution from Gaussian to Lorentzian.[78] It is, therefore, instructive to draw the parallel between interchromophoric spectral jumping in polymers[78] to spectral jumping following a reversible charging event in NCs. Spectral jumping events observed in NCs can be thought of as a discrete change in the nature of the single chromophore or as an establishment of a new chromophoric site. The precise nature of the spectral diffusion statistics is currently still subject to debate.[16,56,78,79] Spectral diffusion has been investigated intensively in static single molecule PL excitation spectroscopy as well as hole burning spectroscopy, where it controls the spectral line shape.[80] Our *dynamic* investigation of spectral diffusion, however, shows clearly that two regimes of ΔE statistics exist, depending on whether or not the underlying electron configuration (the chromophore) changes.

Finally, we return to the question of what actually constitutes the origin of the permanent polarization observed in the dielectric response of virtually all colloidal nanoparticles.[45,46] Shim *et al.* previously distinguished between either variations in the surface ligand potential due to the asymmetric internal bonding geometry, shape asymmetry of the overall colloid, surface strain resulting in piezoelectric effects, and surface localized charges.[46] While the dynamics observed in single NC experiments along with the response of the emission to external static electric fields[4] provides strong evidence for the surface charge model, recent electrostatic force microscopy measurements on CdSe quantum rods which exhibit huge dipole moments led to the conclusion that the permanent polarization results from a lattice distortion within the NC rather than ionization induced surface trap filling.[53] The net result of any of these processes is identical in that a large effective dipole is formed which modifies the optical transition. Yet it is hard to conceive how structural changes of the ionic lattice could give rise to the virtual *independence* of spectral dynamics on temperature over an order of magnitude change in temperature (Fig. 6). Surface reconstruction

due to intrinsic self-healing of the wurtzite lattice can even occur at zero temperature,[81] but one would expect thermally induced lattice distortions and defects to become more prominent at increased temperature. In contrast, the weak thermal activation and strong intensity dependence of spectral diffusion are entirely consistent with a deep surface trap population driven by the external optical excitation. The spectral jumps ΔE observed are typically substantially greater than the thermal energy kT at low temperatures, so that energy conservation leaves only a photoinduced process as the origin of the energetically symmetrical spectral dynamics. Indeed, minimizing the excess in photon energy through resonant excitation of epitaxial quantum dots dramatically reduces spectral diffusion induced line broadening.[58]

Although the surface charge model is instructive, we conclude that most likely a number of effects lead to the effective polarization of the NC. A particularly interesting aspect is the increase of the ionization rate with temperature above 50 K (manifested in the spectral jumping histograms). A similar observation was previously drawn from a consideration of PL intermittency.[19] Increased ionization probability and a larger average spectral shift per ionization event at elevated temperatures could be a signature of internal fields arising from thermally induced lattice distortions,[53] which would accelerate the expulsion of carriers. This process, however, does not modify the static dipole of the NC itself, which is independent of temperature.[46] The study of the spectral dynamics reveals that the spectral jumping exhibits a strongly sublinear dependence on excitation density; in contrast, the spectral jitter is clearly linear in intensity as seen in Fig. 8. Considering a purely photochemically driven rearrangement of charge on the surface of the NC, the linear dependence of spectral jitter on intensity is not surprising. The harder the system is pumped, the further the surface charge can be displaced on average, the broader the ΔE_{Jitter} histogram. In contrast, reversible particle ionization leading to spectral jumping is a partly thermally activated process. Increased pumping of the transition reduces the activation barrier for ionization by, for example, Auger recombination assisted thermal ionization,[82] leading to a sublinear intensity dependence. The spectral jump histogram directly mirrors the spectral dynamics but effectively controls the PL linewidth in a time integrated measurement.[4]

V. CONCLUSIONS

Semiconductor NCs constitute excellent nanoscale emitters for low temperature single particle spectroscopy. They are readily processed from solution, enabling an accurate control of dilution not readily achieved with gas phase grown semiconductor nanostructures. Shape control of the nanostructure introduces a particularly interesting parameter in establishing the origin of spectral dynamics and the general overall emission properties, such as spectral color, linewidth, and lifetime. The spectral dynamics of single elongated NCs can be accurately understood in terms of spatial diffusion of surface charges in the vicinity of the exciton localized at one end of the nanostructure. The spectral shifts, spectral line broadening, phonon coupling, and, in particular, the novel aspects of intensity modulation and spectral jitter are all consistent with a quantum-confined Stark effect originating from strong local dynamic electric fields. Besides providing insight into the intrinsic photophysics of semiconductor nanostructures, our results also suggest that single NCs can be used as extremely sensitive charge detectors to characterize, for example, optoelectronic devices under operation. As the correlation between spectral linewidth and peak position is also clearly seen at room temperature, the spectral rather than the intensity dynamics of single NCs can provide insight into dielectric processes in less well-defined environments such as in large biomolecules. As in the case of single dye molecules, whose fluorescence dynamics at room temperature can be understood in terms of conformational dynamics,[8] which in turn depend on mechanical aspects such as the viscosity of the environment, spectral dynamics of NCs at room temperature can constitute a powerful dielectric probe.

Note added in proof. Recently, Rothenberg *et al.* reported a correlation between fluorescence intensity and peak position in the spectral diffusion of pure CdSe nanorods.[83]

ACKNOWLEDGMENTS

We are grateful to W. Stadler, A. Helfrich, and C. Holopirek for technical assistance and thank the DFG for financial support through the Sonderforschungsbereich 486 and the Gottfried-Wilhelm-Leibniz Preis. J. L. thanks Dr. Frank Wilhelm for interesting discussions.

*Corresponding author. Dr. John M. Lupton; FAX: +49-89-2180-3441; Email address: john.lupton@physik.uni-muenchen.de

[1] D. Gammon, E. S. Snow, B. V. Shanabrook, D. S. Katzer, and D. Park, Science **273**, 87 (1996); R. Leon, P. M. Petroff, D. Leonard, and S. Fafard, *ibid.* **267**, 1966 (1995).

[2] A. J. Shields, R. M. Stevenson, R. M. Thompson, M. B. Ward, Z. Yuan, B. E. Kardynal, P. See, I. Farrer, C. Lobo, K. Cooper, and D. A. Ritchie, Phys. Status Solidi B **328**, 353 (2003).

[3] M. Nirmal, B. O. Dabbousi, M. G. Bawendi, J. J. Macklin, J. K. Trautman, T. D. Harris, and L. E. Brus, Nature (London) **383**, 802 (1996).

[4] S. A. Empedocles, R. Neuhauser, K. Shimizu, and M. G. Bawendi, Adv. Mater. (Weinheim, Ger.) **11**, 1243 (1999).

[5] S. A. Empedocles, D. J. Norris, and M. G. Bawendi, Phys. Rev. Lett. **77**, 3873 (1996).

[6] W. E. Moerner, Science **265**, 46 (1994).

[7] D. M. Adams, L. Brus, C. E. D. Chidsey, S. Creager, C. Creutz, C. R. Kagan, P. V. Kamat, M. Lieberman, S. Lindsay, R. A. Marcus, R. M. Metzger, M. E. Michel-Beyerle, J. R. Miller, M. D. Newton, D. R. Rolison, O. Sankey, K. S. Schanze, J. Yardley, and X. Y. Zhu, J. Phys. Chem. B **107**, 6668 (2003).

[8] H. P. Lu and X. S. Xie, Nature (London) **385**, 143 (1997).

[9] R. A. L. Vallee, M. Van Der Auweraer, F. C. De Schryver, D. Beljonne, and M. Orrit, ChemPhysChem **6**, 81 (2005).
[10] M. Lippitz, F. Kulzer, and M. Orrit, ChemPhysChem **6**, 770 (2005).
[11] W. E. Moerner and M. Orrit, Science **283**, 1670 (1999).
[12] R. Zondervan, F. Kulzer, S. B. Orlinskii, and M. Orrit, J. Phys. Chem. A **107**, 6770 (2003).
[13] M. Cotlet, S. Masuo, G. B. Luo, J. Hofkens, M. Van der Auweraer, J. Verhoeven, K. Müllen, X. L. S. Xie, and F. De Schryver, Proc. Natl. Acad. Sci. U.S.A. **101**, 14343 (2004).
[14] R. Gronheid, A. Stefan, M. Cotlet, J. Hofkens, J. Q. Qu, K. Mullen, M. Van der Auweraer, J. W. Verhoeven, and F. C. De Schryver, Angew. Chem., Int. Ed. **42**, 4209 (2003).
[15] A. P. Alivisatos, Science **271**, 933 (1996).
[16] R. G. Neuhauser, K. T. Shimizu, W. K. Woo, S. A. Empedocles, and M. G. Bawendi, Phys. Rev. Lett. **85**, 3301 (2000).
[17] M. Kuno, D. P. Fromm, S. T. Johnson, A. Gallagher, and D. J. Nesbitt, Phys. Rev. B **67**, 125304 (2003).
[18] B. R. Fisher, H. J. Eisler, N. E. Stott, and M. G. Bawendi, J. Phys. Chem. B **108**, 143 (2004).
[19] U. Banin, M. Bruchez, A. P. Alivisatos, T. Ha, S. Weiss, and D. S. Chemla, J. Chem. Phys. **110**, 1195 (1999).
[20] R. Verberk, A. M. van Oijen, and M. Orrit, Phys. Rev. B **66**, 233202 (2002).
[21] J. G. Müller, U. Lemmer, G. Raschke, M. Anni, U. Scherf, J. M. Lupton, and J. Feldmann, Phys. Rev. Lett. **91**, 267403 (2003).
[22] G. Schlegel, J. Bohnenberger, I. Potapova, and A. Mews, Phys. Rev. Lett. **88**, 137401 (2002).
[23] X. Brokmann, J. P. Hermier, G. Messin, P. Desbiolles, J. P. Bouchaud, and M. Dahan, Phys. Rev. Lett. **90**, 120601 (2003).
[24] M. Kuno, D. P. Fromm, H. F. Hamann, A. Gallagher, and D. J. Nesbitt, J. Chem. Phys. **112**, 3117 (2000).
[25] S. Hohng and T. Ha, J. Am. Chem. Soc. **126**, 1324 (2004).
[26] M. Bruchez, M. Moronne, P. Gin, S. Weiss, and A. P. Alivisatos, Science **281**, 2013 (1998).
[27] W. C. W. Chan and S. M. Nie, Science **281**, 2016 (1998).
[28] M. E. Pistol, Phys. Rev. B **63**, 113306 (2001).
[29] V. I. Klimov, A. A. Mikhailovsky, D. W. McBranch, C. A. Leatherdale, and M. G. Bawendi, Science **287**, 1011 (2000).
[30] S. A. Empedocles and M. G. Bawendi, J. Phys. Chem. B **103**, 1826 (1999).
[31] S. A. Empedocles and M. G. Bawendi, Science **278**, 2114 (1997).
[32] R. J. Warburton, C. Schaflein, D. Haft, F. Bickel, A. Lorke, K. Karrai, J. M. Garcia, W. Schoenfeld, and P. M. Petroff, Nature (London) **405**, 926 (2000).
[33] W. Heller, U. Bockelmann, and G. Abstreiter, Phys. Rev. B **57**, 6270 (1998).
[34] G. W. Wen, J. Y. Lin, H. X. Jiang, and Z. Chen, Phys. Rev. B **52**, 5913 (1995).
[35] J. Seufert, M. Obert, M. Rambach, G. Bacher, A. Forchel, T. Passow, K. Leonardi, and D. Hommel, Physica E (Amsterdam) **13**, 147 (2002).
[36] H. Gotoh, H. Kamada, H. Ando, and J. Temmyo, Appl. Phys. Lett. **76**, 867 (2000).
[37] T. Arakawa, Y. Kato, F. Sogawa, and Y. Arakawa, Appl. Phys. Lett. **70**, 646 (1997).
[38] H. X. Fu, Phys. Rev. B **65**, 045320 (2002).
[39] A. Franceschetti and A. Zunger, Phys. Rev. B **62**, 2614 (2000).
[40] E. Menendez-Proupin and C. Trallero-Giner, Phys. Rev. B **69**, 125336 (2004).
[41] D. A. B. Miller, D. S. Chemla, T. C. Damen, A. C. Gossard, W. Wiegmann, T. H. Wood, and C. A. Burrus, Phys. Rev. Lett. **53**, 2173 (1984).
[42] L. W. Wang, J. Phys. Chem. B **105**, 2360 (2001).
[43] D. A. B. Miller, J. S. Weiner, and D. S. Chemla, IEEE J. Quantum Electron. **22**, 1816 (1986).
[44] K. T. Shimizu, W. K. Woo, B. R. Fisher, H. J. Eisler, and M. G. Bawendi, Phys. Rev. Lett. **89**, 117401 (2002).
[45] S. A. Blanton, R. L. Leheny, M. A. Hines, and P. Guyot-Sionnest, Phys. Rev. Lett. **79**, 865 (1997).
[46] M. Shim and P. Guyot-Sionnest, J. Chem. Phys. **111**, 6955 (1999).
[47] B. C. Hess, I. G. Okhrimenko, R. C. Davis, B. C. Stevens, Q. A. Schulzke, K. C. Wright, C. D. Bass, C. D. Evans, and S. L. Summers, Phys. Rev. Lett. **86**, 3132 (2001).
[48] A. Hasselbarth, A. Eychmueller, and H. Weller, Chem. Phys. Lett. **203**, 271 (1993).
[49] T. D. Krauss, S. O'Brien, and L. E. Brus, J. Phys. Chem. B **105**, 1725 (2001).
[50] T. D. Krauss and L. E. Brus, Phys. Rev. Lett. **83**, 4840 (1999).
[51] M. Shim, S. V. Shilov, M. S. Braiman, and P. Guyot-Sionnest, J. Phys. Chem. B **104**, 1494 (2000).
[52] D. S. Ginger, A. S. Dhoot, C. E. Finlayson, and N. C. Greenham, Appl. Phys. Lett. **77**, 2816 (2000).
[53] R. Krishnan, M. A. Hahn, Z. Yu, J. Silcox, P. M. Fauchet, and T. D. Krauss, Phys. Rev. Lett. **92**, 216803 (2004).
[54] L. S. Li and A. P. Alivisatos, Phys. Rev. Lett. **90**, 097402 (2003).
[55] X. G. Peng, L. Manna, W. D. Yang, J. Wickham, E. Scher, A. Kadavanich, and A. P. Alivisatos, Nature (London) **404**, 59 (2000).
[56] J. Müller, J. M. Lupton, A. L. Rogach, J. Feldmann, D. V. Talapin, and H. Weller, Phys. Rev. Lett. **93**, 167402 (2004).
[57] C. Kammerer, C. Voisin, G. Cassabois, C. Delalande, P. Roussignol, F. Klopf, J. P. Reithmaier, A. Forchel, and J. M. Gerard, Phys. Rev. B **66**, 041306(R) (2002).
[58] M. Bayer and A. Forchel, Phys. Rev. B **65**, 041308(R) (2002).
[59] P. Palinginis, S. Tavenner, M. Lonergan, and H. L. Wang, Phys. Rev. B **67**, 201307(R) (2003).
[60] J. Seufert, R. Weigand, G. Bacher, T. Kummell, A. Forchel, K. Leonardi, and D. Hommel, Appl. Phys. Lett. **76**, 1872 (2000).
[61] L. Besombes, K. Kheng, L. Marsal, and H. Mariette, Phys. Rev. B **65**, 121314(R) (2002).
[62] H. D. Robinson and B. B. Goldberg, Phys. Rev. B **61**, R5086 (2000).
[63] B. Patton, W. Langbein, and U. Woggon, Phys. Rev. B **68**, 125316 (2003).
[64] V. Türck, S. Rodt, O. Stier, R. Heitz, R. Engelhardt, U. W. Pohl, D. Bimberg, and R. Steingruber, Phys. Rev. B **61**, 9944 (2000).
[65] P. G. Blome, M. Wenderoth, M. Hübner, R. G. Ulbrich, J. Porsche, and F. Scholz, Phys. Rev. B **61**, 8382 (2000).
[66] J. Seufert, M. Obert, M. Scheibner, N. A. Gippius, G. Bacher, A. Forchel, T. Passow, K. Leonardi, and D. Hommel, Appl. Phys. Lett. **79**, 1033 (2001).
[67] D. V. Talapin, R. Koeppe, S. Gotzinger, A. Kornowski, J. M. Lupton, A. L. Rogach, O. Benson, J. Feldmann, and H. Weller, Nano Lett. **3**, 1677 (2003).
[68] H. Htoon, P. J. Cox, and V. I. Klimov, Phys. Rev. Lett. **93**, 187402 (2004).
[69] A. Kiraz, M. Ehrl, C. Brauchle, and A. Zumbusch, J. Chem. Phys. **118**, 10821 (2003).

[70] M. B. Weissman, Rev. Mod. Phys. **60**, 537 (1988).
[71] S. W. Jung, T. Fujisawa, Y. Hirayama, and Y. H. Jeong, Appl. Phys. Lett. **85**, 768 (2004).
[72] H. Htoon, M. J. O'Connell, S. K. Doorn, and V. I. Klimov, Phys. Rev. Lett. **94**, 127403 (2005).
[73] D. Kulik, H. Htoon, C. K. Shih, and Y. D. Li, J. Appl. Phys. **95**, 1056 (2004).
[74] E. Paladino, L. Faoro, G. Falci, and R. Fazio, Phys. Rev. Lett. **88**, 228304 (2002).
[75] G. Falci, A. D'Arrigo, A. Mastellone, and E. Paladino, Phys. Rev. Lett. **94**, 167002 (2005).
[76] G. Bacher, A. A. Maksimov, H. Schomig, V. D. Kulakovskii, M. K. Welsch, A. Forchel, P. S. Dorozhkin, A. V. Chernenko, S. Lee, M. Dobrowolska, and J. K. Furdyna, Phys. Rev. Lett. **89**, 127201 (2002).
[77] P. F. Barbara, A. J. Gesquiere, S. J. Park, and Y. L. Lee, Acc. Chem. Res. **38**, 602 (2005).
[78] F. Schindler, J. M. Lupton, J. Feldmann, and U. Scherf, Proc. Natl. Acad. Sci. U.S.A. **101**, 14695 (2004).
[79] F. Schindler and J. M. Lupton, ChemPhysChem **6**, 926 (2005).
[80] Y. J. Jung, E. Barkai, and R. J. Silbey, J. Chem. Phys. **117**, 10980 (2002).
[81] A. Puzder, A. J. Williamson, F. Gygi, and G. Galli, Phys. Rev. Lett. **92**, 217401 (2004).
[82] R. M. Kraus, P. Lagoudakis, J. Müller, A. L. Rogach, J. M. Lupton, J. Feldmann, D. V. Talapin, and H. Weller, J. Phys. Chem. B **109**, 18214 (2005).
[83] E. Rothenberg, M. Kazes, E. Shaviv, and U. Banin, Nano Lett. **5**, 1581 (2005).